Journal of Visualized Experiments

A Three-dimensional Model of Spheroids to Study Colon Cancer Stem Cells

--Manuscript Draft--

Article Type:	Methods Article - JoVE Produced Video
Manuscript Number:	JoVE61783R2
Full Title:	A Three-dimensional Model of Spheroids to Study Colon Cancer Stem Cells
Corresponding Author:	Michelina Plateroti Centre de Recherche en Cancerologie de Lyon Lyon, Rhone FRANCE
Corresponding Author's Institution:	Centre de Recherche en Cancerologie de Lyon
Corresponding Author E-Mail:	michelina.plateroti@univ-lyon1.fr
Order of Authors:	Maria Virginia Giolito
	Léo Claret
	Carla Frau
	Michelina Plateroti
Additional Information:	
Question	**Response**
Please indicate whether this article will be Standard Access or Open Access.	Standard Access (US$2,400)
Please indicate the **city, state/province, and country** where this article will be **filmed**. Please do not use abbreviations.	Strasbourg, France
Please confirm that you have read and agree to the terms and conditions of the author license agreement that applies below:	I agree to the Author License Agreement
Please specify the section of the submitted manuscript.	Cancer Research
Please provide any comments to the journal here.	1-I don’t know «who assisted me in submitting this manuscript». In the list, Dr Upponi seems to be the only specialist in Oncology. 2-I uploaded the cover letter as «supplementary file».

TITLE:

A Three-dimensional Model of Spheroids to Study Colon Cancer Stem Cells

AUTHORS AND AFFILIATIONS:

Maria Virginia Giolito[1,#], Léo Claret[1,#], Carla Frau and Michelina Plateroti*[,1,#]

[1]Centre de Recherche en Cancérologie de Lyon, INSERM U1052, CNRS UMR5286, Université de Lyon, Université Lyon 1, Centre Léon Bérard, Département de la recherche, 69000 Lyon, France

Maria Virginia Giolito (maria-virginia.giolito@inserm.fr)
Léo Claret (leo.claret@inserm.fr)
Carla Frau (carla.frau@inserm.fr)

***Corresponding author**
Michelina Plateroti
Centre de Recherche en Cancérologie de Lyon (CRCL)
28 Rue Laennec, 69373 Lyon, France
Tel: 33 4 69166617
Fax: 33 4 78782720
E-mail: michelina.plateroti@univ-lyon1.fr

[#]Current address
UMR-S1113-IRFAC
INSERM, Université de Strasbourg
3 avenue Molière, 67200 Strasbourg, France
Tel: 33 3 88 27 77 27
E-mail: plateroti@unistra.fr

KEYWORDS:

Caco2 cells, Cancer stem cells, Cell proliferation, Colon cancer, Colonospheres, Colonospheres growth

SUMMARY:

This protocol presents a novel, robust, and reproducible culture system to generate and grow three-dimensional spheroids from Caco2 colon adenocarcinoma cells. The results provide the first proof-of-concept for the appropriateness of this approach to study cancer stem cell biology, including the response to chemotherapy.

ABSTRACT:

Colorectal cancers are characterized by heterogeneity and a hierarchical organization comprising a population of cancer stem cells (CSCs) responsible for tumor development, maintenance, and resistance to drugs. A better understanding of CSC properties for their specific targeting is, therefore, a pre-requisite for effective therapy. However, there is a paucity of suitable preclinical models for in-depth investigations. Although in vitro two-dimensional (2D) cancer cell lines provide valuable insights into tumor biology, they do not replicate the phenotypic and genetic tumor heterogeneity. In contrast, three-dimensional (3D) models address and reproduce near-physiological cancer complexity and cell heterogeneity. The aim of this work was to design a robust and reproducible 3D culture system to study CSC biology. The present methodology describes the development and optimization of conditions to generate 3D spheroids, which are homogenous in size, from Caco2 colon adenocarcinoma cells, a model that can be used for long-term culture. Importantly, within the spheroids, the cells which were organized around lumen-like structures, were characterized by differential cell proliferation patterns and by the presence of CSCs expressing a panel of markers. These results provide the first proof-of-concept for the appropriateness of this 3D approach to study cell heterogeneity and CSC biology, including the response to chemotherapy.

INTRODUCTION:

Colorectal cancer (CRC) remains the second leading cause of cancer-associated deaths in the world[1]. The development of CRC is the result of a progressive acquisition and accumulation of genetic mutations and/or epigenetic alterations[2,3], including the activation of oncogenes and inactivation of tumor suppressor genes[3,4]. Moreover, non-genetic factors (e.g., the microenvironment) can contribute to and promote oncogenic transformation and thus participate in the evolution of CRCs[5]. Importantly, CRCs are composed of different cell populations, including undifferentiated CSCs and bulk tumor cells displaying some differentiation traits, which constitute a hierarchical structure reminiscent of the organization of the epithelium in a normal colon crypt[6,7].

CSCs are considered to be responsible for tumor appearance[8], its maintenance and growth, metastatic capacity, and resistance to conventional therapies[6,7]. Within tumors, cancer cells, including CSCs, display a high level of heterogeneity and complexity in terms of their distinct mutational and epigenetic profiles, morphological and phenotypic differences, gene expression, metabolism, proliferation rates, and metastatic potential[9]. Therefore, to better understand cancer biology, tumor progression, and acquisition of resistance to therapy and its translation into effective treatments, human preclinical models capturing this cancer heterogeneity and hierarchy are important[10,11].

In vitro 2D cancer cell lines have been used for a long time and provide valuable insights into tumor development and the mechanisms underlying the efficacy of therapeutic molecules. However, their limitation with respect to the lack of the phenotypic and genetic heterogeneity found in the original tumors is now widely recognized[12]. Moreover, nutrients, oxygen, pH

gradients, and the tumor microenvironment are not reproduced, the microenvironment being especially important for the maintenance of different cell types including CSCs[11,12]. To overcome these main drawbacks, several 3D models have been developed to experimentally address and reproduce the complexity and heterogeneity of cancers. In effect, these models recapitulate tumor cellular heterogeneity, cell-cell interactions, and spatial architecture, similar to those observed in vivo[12–14]. Primary tumor organoids established from fresh tumors, as well as cell line-derived spheroids, are largely employed[15,16].

Spheroids can be cultured in a scaffold-free or scaffold-based manner to force the cells to form and grow in cell aggregates. Scaffold-free methods are based on the culture of cells under non-adherent conditions (e.g., the hanging-drop method or ultra-low attachment plates), whereas scaffold-based models rely on natural, synthetic, or hybrid biomaterials to culture cells[12–14]. Scaffold-based spheroids present different disadvantages as the final spheroid formation will depend on the nature and composition of the (bio)material used. Although the scaffold-free spheroid methods available so far do not rely on the nature of the substrate, they generate spheroids that vary in structure and size[17,18].

This work was aimed at designing a robust and reproducible 3D culture system of spheroids, which are homogenous in size, composed of Caco2 colon adenocarcinoma cells to study CSC biology. Caco2 cells are of particular interest owing to their capacity to differentiate over time[19,20], strongly suggesting a stem-like potential. Accordingly, long-term culture of the spheroids revealed the presence of different CSC populations with different responses to chemotherapy.

PROTOCOL:

NOTE: The details of all reagents and materials are listed in the **Table of Materials**.

1. Spheroid formation

1.1. Spheroid culture media

1.1.1. Prepare basal medium consisting of Dulbecco's Modified Eagle Medium (DMEM) supplemented with 4 mM L-alanyl-L-glutamine dipeptide.

1.1.2. Prepare DMEM complete medium containing 10% fetal bovine serum (FBS) and 1% penicillin-streptomycin (Pen/Strep) in basal medium from step 1.1.1.

1.1.3. Prepare DMEM/basement membrane matrix medium containing 2.5% basement membrane matrix, 10% FBS, and 1% Pen/Strep in basal medium from step 1.1.1.

1.2. Preparation of plates for spheroid formation

1.2.1. Warm basal and DMEM/basement membrane matrix medium at room temperature (RT) for approximately 20 min.

1.2.2. Pretreat the wells of a 24-well plate dedicated to spheroid formation by adding 500 µL of anti-adherence rinsing solution to each well.

NOTE: In these plates, each well consists of 1,200 microwells.

1.2.3. Centrifuge the plate at 1,200 × *g* for 5 min in a swinging bucket rotor with adaptors for plates.

NOTE: If only one plate is used, prepare an additional standard plate filled with water to counterbalance the weight.

1.2.4. Rinse each well with 2 mL of warm basal medium, and aspirate the medium from the wells.

1.2.5. Observe the plate under the microscope to ensure that bubbles have been completely removed from the microwells. If bubbles remain trapped, centrifuge again at 1,200 × *g* for 5 min to eliminate the bubbles.

1.2.6. Repeat the rinsing steps 1.2.4–1.2.5.

1.2.7. Add 1 mL of warm DMEM/basement membrane matrix medium to each well.

1.3. Generation of spheroids

1.3.1. Grow the Caco2 cells in a 2D monolayer in DMEM medium supplemented with 10% FBS and 1% Pen/Strep at 37 °C in a humidified atmosphere containing 5% CO_2 (hereafter referred to as 37 °C/5% CO_2).

NOTE: The maximum number of cell passages to be used is 80.

1.3.2. When 80% of confluency is reached, wash the cells with phosphate-buffered saline (PBS) 1x (5 mL for a 10 cm dish), add trypsin-ethylenediamine tetraacetic acid (EDTA) (2 mL for a 10 cm dish), and incubate for 2–5 min at 37 °C/5% CO_2.

1.3.3. Check cell detachment under the microscope, and neutralize the trypsin by adding 4 mL of DMEM complete medium per 10 cm dish.

1.3.4. Count cells using a hemocytometer to determine the total number of cells.

1.3.5. Centrifuge the cell suspension at 1,200 × *g* for 3 min. Discard the supernatant, and

resuspend the pellet in an appropriate volume of DMEM/basement membrane matrix medium.

1.3.6. Refer to **Table 1** to determine the number of cells required per well to achieve the desired number of cells per microwell. Alternatively, calculate the number of cells using the following formula for a 24-well plate, considering each well contains 1,200 microwells*:*

Required number of cells per well = Desired number of cells per microwell × 1,200

1.3.7. Add the required volume of the cell suspension to each well to achieve the desired cell number in a final volume of 1 mL.

1.3.8. Add 1 mL of DMEM/basement membrane matrix medium to each well to reach the final volume of 2 mL per well (see also step 1.2.7).

NOTE: Be careful not to introduce bubbles into the microwells.

1.3.9. Centrifuge the plate immediately at 1,200 × *g* for 5 min to capture the cells in the microwells. If necessary, counterbalance the centrifuge with a standard plate filled with water.

1.3.10. Observe the plate under the microscope to verify that the cells are evenly distributed among the microwells.

1.3.11. Incubate the plate at 37 °C/5% CO_2 for 48 h without disturbing the plate.

NOTE: According to the original protocol[21], although many cell lines can form spheroids within 24 h, some require a longer incubation time. In this protocol, 48 h are sufficient for spheroid formation.

1.4. Harvesting the spheroids from the microwells

1.4.1. Warm the basal and DMEM/basement membrane matrix medium at RT for approximately 20 min.

1.4.2. Using a serological pipette, remove half of the culture medium (1 mL) from each well.

1.4.3. Add the medium back onto the surface of the well to dislodge the spheroids from the microwells.

NOTE: Do not touch or triturate the spheroids.

1.4.4. Place a 37 µm reversible strainer (or a 40 µm standard strainer) on the top of a 50 mL conical tube to collect the spheroids.

NOTE: If using a 40 µm standard strainer, place it upside down.

1.4.5. Gently aspirate the dislodged spheroids (from step 1.4.3), and pass the spheroid suspension through the strainer.

NOTE: The spheroids will remain on the filter; single cells will flow through with the medium.

1.4.6. Using a serological pipette, dispense 1 mL of the warm basal medium across the entire surface of the well to dislodge any remaining spheroids and recover them on the strainer.

1.4.7. Repeat this washing step 1.4.6 twice.

1.4.8. Observe the plate under the microscope to ensure that all spheroids have been removed from the wells. Repeat the wash if necessary (steps 1.4.6–1.4.7).

1.4.9. Invert the strainer, and place it on a new 50 mL conical tube. Collect the spheroids by washing the strainer with DMEM/basement membrane matrix medium.

NOTE: The collected spheroids are ready for downstream applications and analyses.

1.5. Long-term culture of spheroids

1.5.1. Prepare 1.5% agarose solution in basal medium, and sterilize it by autoclaving (standard cycle).

1.5.2. While the agarose solution is warm and still liquid, coat the wells of standard culture plates or dishes, as described in **Table 2**.

NOTE: Warming the dish/plate in the oven will facilitate the coating step. Coated dishes/plates can be left at RT for up to 10 days in a sterile environment and protected from the light.

1.5.3. Seed the harvested spheroids (from step 1.4.9) in the agarose-coated plates, and add DMEM/basement membrane matrix medium to achieve the final volume depending on the size of the plate.

NOTE: To avoid spheroid aggregates, seed them at the optimal density of 22 spheroids/cm^2. Observe that the coating is not perfectly flat, and it rises towards the edge, creating a light concavity at the center of the plate. If the number of spheroids is too high, they are more likely to adhere to each other.

1.5.4. Incubate the plate at 37 °C/5% CO_2 until recovery of the spheroids for specific analyses.

1.6. Treatment of spheroids with chemotherapeutic drugs

1.6.1. Plate spheroids from step 1.5.4, and grow them for 2 days. Starting from day 3 (D3), treat

them with FOLFIRI (5-Fluorouracil, 50 µg/mL; Irinotecan, 100 µg/mL; Leucovorin, 25 µg/mL) or with FOLFOX (5-Fluorouracil, 50 µg/mL; Oxaliplatin, 10 µg/mL; Leucovorin, 25 µg/mL) chemotherapeutic regimen combinations routinely used to treat CRC patients[22–25], or maintain them in (control) not-treated (NT) condition.

1.6.2. Collect the spheroids after 3 days of treatment by using a pipette with the tip cut off (1,000 µL tip), ensuring that each condition is represented by at least three replicates. Centrifuge them at 1,000 × *g* for 3 min, and then remove the supernatant.

1.6.3. Fix the pellets in 2% paraformaldehyde (PFA) for histological analysis (see section 3), or use the pellets for RNA extraction (see section 4).

1.6.4. To analyze cell death, incubate the spheroids from step 1.6.1 in black culture well plates in DMEM/basement membrane matrix medium for 30 min with a nucleic acid stain (1:5000 dilution) that does not permeate live cells, but penetrates the compromised membranes of dead cells[26]. Measure the accumulation of fluorescence with a microplate reader.

2. **Monitoring spheroid growth**

2.1. Using an inverted microscope, acquire representative images of spheroids maintained under different conditions throughout the days in culture.

2.2. Analyze the images by measuring three different representative diameters of each spheroid using appropriate software.

2.3. Use the following formula to obtain the estimated sphere volume.

$$\text{Estimated volume } (\mu m^3) = \frac{4}{3}\pi \left(\frac{d_1}{2}\frac{d_2}{2}\frac{d_3}{2}\right)$$

NOTE: The terms, d1, d2, and d3, are the three diameters of the spheroid.

3. **Immunofluorescence (IF) and histological staining**

3.1. Fixation and paraffin embedding

3.1.1. Collect the spheroids at selected time-points using a pipette with the tip cut off as described in step 1.6.2, and fix them for 30 min at RT in 2% PFA.

NOTE: Alternatively, store the samples at this step at 4 °C until further use.

3.1.2. For paraffin embedding, wash the spheroids 3x with PBS 1x, and resuspend them in 70% ethanol. After paraffin inclusion and sectioning, perform hematoxylin & eosin (H&E) staining for histological analysis.

3.2. Immunolabeling of paraffin sections

NOTE: Use 5-μm-thick sections for indirect immunostaining.

3.2.1. Incubate slides at 60 °C for 2 h to melt the wax and improve deparaffinization.

3.2.2. Wash the slides twice for 3 min in methylcyclohexane.

3.2.3. Wash the slides for 3 min in 1:1 methylcyclohexane:100% ethanol.

3.2.4. Wash the slides twice for 3 min in 100% ethanol.

NOTE: Perform all manipulations for step 3.2.2 to step 3.2.4 in a chemical hood.

3.2.5. Wash the slides for 3 min in 90% ethanol.

3.2.6. Wash the slides for 3 min in 75% ethanol.

3.2.7. Wash the slides for 3 min in 50% ethanol.

3.2.8. Wash the slides under tap water.

3.2.9. Rehydrate the slides in distilled water for 5 min.

3.2.10. Prepare 700 mL of 0.01 M citrate buffer, pH 6.0, and add it to a suitable container (width: 11.5 cm, length: 17 cm, height: 7 cm); submerge the slides in it. Heat the container in the microwave for 9–10 min at 700 W, and when the boiling starts, decrease the power to 400–450 W. Incubate for an additional 10 min.

3.2.11. Let the slides cool down in the buffer to RT for approximately 30–40 min.

3.2.12. Wash the slides twice in PBS for 5 min.

3.2.13. Draw a circle around the sections with a marker pen to create a barrier for liquids applied to the sections.

3.2.14. Incubate each section with 50 µL of blocking buffer (10% normal goat serum, 1% bovine serum albumin (BSA), and 0.02% Triton X-100 in PBS) for at least 30 min at RT.

3.2.15. Remove the blocking buffer, and add 50 µL of primary antibodies diluted in the incubation buffer (1% normal goat serum, 0.1% BSA, and 0.02% Triton X-100 in PBS). Incubate for 2 h at RT or overnight at 4 °C.

3.2.16. Remove the primary antibodies, and wash the slides 3x in PBS for 5 min.

3.2.17. Incubate the slides with 50 µL of fluorescent secondary antibodies diluted in the incubation buffer for 1 h at RT.

3.2.18. Remove the secondary antibodies, and wash the slides 3x in PBS for 5 min.

3.2.19. Add 50 µL of mounting medium with 4',6-diamidino-2-phenylindole to each section, and place a glass coverslip over the section.

4. RNA extraction, reverse transcription-polymerase chain reaction (RT-PCR), and quantitative RT-PCR (qRT-PCR)

4.1. Collect spheroids at different time-points, each point represented by at least three replicates. Centrifuge them at 1,000 × *g* for 3 min, and then remove the supernatant.

NOTE: Pellets can be directly used for RNA extraction or stored at -20 °C until further use.

4.2. Isolate the total RNA using a commercial RNA isolation kit, according to the manufacturer's instructions.

4.3. Reverse-transcribe 500 ng of each RNA sample into complementary DNA (cDNA) with a commercial kit according to the manufacturer's instructions.

4.4. After reverse transcription, perform a PCR analysis on 1 µg of cDNA to amplify a housekeeping gene with primers located in different exons.

NOTE: This step enables the verification of the absence of any genomic DNA contamination in the RNA preparations. For this protocol, peptidylprolyl isomerase B (*PPIB)* primers were used.

4.5. Perform qPCR amplification on 4 µg of previously diluted cDNA (1:20 in RNAse-free double-distilled water) by using primers specific for the genes of interest. In each sample, quantify specific mRNA expression by using the ΔΔCt method and values normalized against a housekeeping gene levels.

NOTE: For this protocol, β-actin (*ACTB)* was selected. Primers used in this protocol are listed in **Table 3**.

REPRESENTATIVE RESULTS:

As the lack of homogeneity in the size of spheroids is one of the main drawbacks of currently available 3D spheroid culture systems[13], the aim of this work was to set up a reliable and reproducible protocol to obtain homogenous spheroids. First, to establish ideal working conditions, different numbers of Caco2 cells were tested, ranging from 50 to 2,000 cells per

microwell/spheroid using dedicated plates (**Table 1**). In effect, each well in these plates contains 1,200 microwells, enabling the formation of the same number of spheroids per well, and more importantly, the formation of one spheroid per microwell[21]. After two days of culture, the wells containing 2,000 cells per spheroid grew as a monolayer, and 50 cells per spheroid gave rise to small and non-homogenous spheroids (**Figure 1A**). These two conditions were therefore excluded from further analyses. To establish long-term cultures, spheroids were harvested from the microwells and seeded under non-adherent conditions in freshly prepared agarose-coated plates. Spheroid growth was then monitored throughout the experimental time-course by measuring the change in volume. To take into account the non-spherical shape, three different diameters of each spheroid were measured, and the volume formula was applied[27] (**Figure 1B**). Spheroids generated from 100 and 200 cells maintained their initial size over the entire course of the experiment, whereas those containing 1,000 cells disintegrated during harvesting due to their large size and, consequently, presented more variability in their volume. Therefore, as spheroids arising from 500 cells showed the most homogenous increase in size over the experimental time-course, this number of cells was used for spheroid formation.

Second, besides 500 cells per spheroid, additional cell numbers ranging from 300 to 800 cells were studied. Moreover, to improve the non-adherent conditions, the original protocol was modified by pretreating the wells twice instead of applying only one wash. An improvement in spheroid homogeneity and compaction was observed with these changes (**Figure 2A**). The size of the spheroids in each condition was measured at the time of harvest (**Figure 2B**), and their long-term growth was monitored throughout the days in culture in agarose-coated dishes (**Figure 2C**). Based on the results, 500 and 600 cells/spheroid were confirmed as the optimal conditions yielding good growth and low variability. Owing to the more homogenous growth profile throughout the experimental time-course and the compact structures formed, 600 cells per spheroid was selected as the cell number for subsequent experiments. Finally, to further improve the protocol, DMEM complete medium was supplemented with 2.5% of basement membrane matrix, which contains additional growth factors and a large panel of extracellular matrix proteins[28]. Indeed, the multilobular shape of the spheroids could be due to the lack of signals from the microenvironment that may have affected cell polarization[29,30]. The addition of basement membrane matrix enhanced spheroid growth and improved their homogeneity (**Figure 2D**). An example of this improvement can be seen for 500 cells per spheroid. In the absence of the basement membrane matrix (**Figure 1B**), the size of the spheroids was more heterogeneous, doubling from D3 to D7 and then reaching a plateau. However, in the presence of the basement membrane matrix (**Figure 2C**), the size of the spheroids at each time-point was more homogeneous, increasing proportionally over time.

To analyze long-term features of the spheroids, they were recovered at different time-points after culture in agarose-coated dishes for detailed histological and IF analyses on paraffin sections. H&E staining showed that cells within the spheroids underwent changes in their organization and shape over time. Indeed, cells were densely arranged in multilayers at D3, while flattened cells arranged in monolayers were clearly visible at D10. Interestingly, as indicated by the black dotted lines in the images, a lumen appeared within the spheroids from D5 onwards (**Figure 3**). In parallel, cell proliferation and apoptosis were analyzed by IF using the proliferation

marker, proliferating cell nuclear antigen (PCNA), and the cell death marker, activated caspase 3. Labeling for PCNA revealed that proliferating cells were often present at the outer surface of the spheroids, sometimes in crypt-like or bud-like structures reminiscent of organoid cultures[15]. In addition, a clear increase in PCNA-positive cells at D5 and D7 was observed that declined by D10 (**Figure 4,** left panels). Surprisingly, activated caspase 3 was observed in very few cells in the spheroids at both D3 and D5 (**Figure 4,** left panels) over longer periods of time (data not shown). The expression pattern of β-catenin was also evaluated in paraffin sections. Interestingly, high levels of *β*-catenin expression were observed at each time-point with clear membrane-bound and cytoplasmic staining (**Figure 4**, right panels). Membrane-bound β-catenin participates in cell-cell adhesion by binding to E-cadherin[31]. A high level of β-catenin labeling was noted in clusters of cells at all time-points. In some cases, cells also displayed clear nuclear β-catenin localization (**Figure 4**, right panels). Caco2 cells are known to differentiate in vitro in 2D mainly into enterocytes[19,32]. However, the expression of differentiation markers, such as chromogranin A (enteroendocrine cells), lysozyme (Paneth cells) or mucin 2 (MUC 2, goblet cells), was undetectable in these spheroids by IF (data not shown). However, the potential to differentiate into enterocytes was confirmed, given that the spheroids expressed *ALPI* (alkaline phosphatase) and solute carrier family 2, transcript variant 2 (*SLC2A5)/*glucose transporter 5 (*GLUT5*) mRNAs (**Figure 5**). These mRNA levels increased at D5 and D7, but the difference was either not significant (*ALPI*) or only marginally significant (*SLC2A5*) compared to the levels at D3.

With the final aim of defining whether the spheroids generated and cultured based on this new method are a reliable tool to study CSCs, the expression of CSC markers was analyzed by IF and qRT-PCR. Cluster of differentiation (CD)133 and CD44 characterize cancer cell populations including CSCs[7,33,34] and are also expressed by SCs in the normal intestine and colon[33–35]. Clusters of CD133-positive cells were mainly localized on the external surface of the spheroids at each time-point (**Figure 6A,** left panels). CD44-positive cells were less frequent, but were always associated with CD133-positive cells (**Figure 6A,** right panels), indicating the existence of a population of CD133/CD44 double-positive CSC-like cells and a population expressing only CD133. Olfactomedin 4 (OLFM4) and Musashi 1 (MSI1) were examined as SC/CSC markers; these markers are expressed in a very limited manner in colon crypts[36,37] and also in distinct cell populations[35,38]. Only a few MSI1-positive cells were observed at each time-point (**Figure 7**), whereas OLFM4 remained undetectable (data not shown). Nevertheless, as observed for CD44 and CD133, MSI1-labeled cells were located on the external surface of the spheroids in crypt-like or bud-like structures. The same markers were also analyzed at the mRNA level at the same time-points after culture in agarose-coated dishes. Aldehyde dehydrogenase 1 (*ALDH1a1*), a well-characterized marker of CSCs[39,40], was also included in the study (**Figure 8**). The analysis of prominin-1 (*PROM1* encoding for CD133) and *CD44* mRNAs confirmed the expression of both markers in spheroids at all time-points analyzed. Of note, however, while *PROM1* mRNA levels were quite similar over time in culture, *CD44* levels decreased from D3 onwards. The difference, however, was only marginally significant when comparing the mRNA levels of D10 and D3.

The analysis of *MSI1* mRNA confirmed its expression in spheroids at each time-point, with significantly higher levels at D3 and D5 compared with those at D7 or D10 (**Figure 8**), whereas *OLFM4* mRNA was not detectable (not shown). Finally, *ALDH1a1* mRNA was expressed in

spheroids at each time-point and showed an expression profile that declined at D10, the levels being only marginally significant compared to those at D3 (**Figure 8**). To validate the appropriateness of the new model to study cancer cell biology, the response to chemotherapy was analyzed in spheroids treated with FOLFOX or FOLFIRI, combination therapies routinely administered to CRC patients[22–25]. First, the efficacy of the treatments in inducing cell death was examined by incubating the spheroids with a fluorescent nucleic acid stain that specifically enters dead cells[26]. Compared to the control NT condition, the treatment with each of the drugs induced significant cell death measured by the accumulation of fluorescence (**Figure 9A**). This observation was also confirmed at the morphological level using live microscopy, which showed that the treatments strongly affected the size and the appearance of the spheroids (**Figure 9B**). Finally, the expression of SC/CSC markers was analyzed by qRT-PCR in spheroids under the same conditions (**Figure 9C**). Intriguingly, a significant decrease in *PROM1* mRNA levels under both FOLFOX and FOLFIRI conditions was observed in comparison to the levels for the control, whereas *MSI1* levels were not affected by the treatments. Furthermore, whereas FOLFOX had no effect on *ALDH1α1* mRNA expression compared to the control, treatment with FOLFIRI significantly increased its levels. *OLFM4* mRNA was not detected, and *CD44* mRNA levels were extremely low (data not shown).

FIGURE AND TABLE LEGENDS:

Figure 1: Setup of spheroid cultures. (**A**) Spheroid formation initiated from the indicated concentrations of Caco2 cells p*er* spheroid/microwell. The top panel shows a representative image of a whole culture plate after two days of culture. The bottom panel shows images of selected microwells per condition. Images were taken at 4x magnification (microwell size: 400 μm). Scale bars: low magnification, 100 μm; high magnification, 30 μm. (**B**) Growth characteristics of the spheroids generated from different number of cells per microwell and analyzed at different time-points. Note that the indicated days include the first two days of culture in the microwells and the subsequent culture of the harvested spheroids in agarose-coated plates. Histograms show mean ± standard deviation, n = 4–6. Black circles show the values for individual spheroids. The formula for the estimated volume is shown in the upper part of the panel, where d1, d2, and d3 indicate the three diameters measured for each spheroid.

Figure 2: Optimization of the conditions for spheroid formation and culture. (**A**) Representative images of spheroids at D7 after their recovery from the microwells (2 days) and culture in agarose-coated dishes (5 days), using new well preparation and culture medium conditions. Scale bar: 30 μm. (**B**) Estimated volume of the freshly harvested spheroids two days after the start of cell culture in the microwells. Histograms show mean ± standard deviation (SD), n = 4–6. Black circles indicate the size of the individual spheroids. (**C**) Estimated volume of the spheroids in long-term culture based on the newly selected conditions. Graphs show the growth characteristics of the spheroids generated from different number of cells per spheroid and analyzed at different time-points after their harvesting, as indicated. Histograms show mean ± SD, n = 6–10. Black circles indicate the size of the individual spheroids. (**D**) Representative images of the chosen 600 cells per spheroid condition over the experimental time-course (right panels) and within the

microwells (left panel). Images were taken at 4x magnification. Scale bars: low magnification, 100 μm; high magnification, 30 μm.

Figure 3: Histological characterization of the spheroids. Histological hematoxylin and eosin (H&E) staining of paraffin sections. Representative images of spheroids at the indicated time-points after harvesting, as indicated. Black dotted lines in each high magnification inset delimit the lumen within the spheroids. Scale bars: low magnification, 30 μm; high magnification, 10 μm.

Figure 4: Caco2 spheroid characterization by immunolabeling. Immunostaining of spheroids for proliferation marker, proliferating cell nuclear antigen (PCNA, red), and cell death marker, activated caspase 3 (green) (left panels) and for β-catenin (red) (right panels) at the indicated times. Images show merged labeling of PCNA (red), activated caspase 3 (green), and nuclei (blue) or of β-catenin (red) and nuclei (blue). White arrows point to cells or groups of cells expressing high levels of β-catenin. Images were taken with a 20x objective. Scale bar: 5 μm.

Figure 5: Analysis of enterocyte differentiation markers by qRT-PCR. Analysis of *ALPI* and *SLC2A5* encoding alkaline phosphatase and GLUT5 proteins, respectively. Histograms show mean ± standard deviation, n = 3, after normalization against *ACTB*. Data are represented as fold change relative to normal colon mucosa (red line = 1). NS: not significant; MS: marginally significant compared with D3 by unpaired Student's *t*-test. Abbreviations: qRT-PCR = quantitative reverse transcription-polymerase chain reaction; GLUT5 = glucose transporter 5; SLC2A5 = solute carrier family 2, transcript variant 2; ACTB = β-actin.

Figure 6: Heterogeneous expression of stem cell markers,CD44 and CD133, in the spheroids. Immunostaining for the stem cell markers, CD133 and CD44, at the indicated times. Images in the left panels show merged labeling of CD133 (green) and nuclei (blue); the same images in the right panels show merged labeling of CD44 (red) and nuclei (blue). Green arrows in the left panels point to CD133-expressing cells, and white arrows in both panels point to cells or groups of cells expressing CD44 and CD133. Images were acquired with a 20x objective. Scale bar: 5 μm.

Figure 7: Heterogeneous expression of stem cell marker, MSI1, in the spheroids. Immunostaining for the stem cell marker MSI1 (red) at the indicated times. Images show merged labeling of MSI1 (red) and nuclei (blue). White dotted lines underline some crypt-like structures where cells are positive for MSI1 immunolabeling. Images were taken at 20x magnification. Scale bar: 5 μm. Abbreviation = MSI1 = Musashi 1.

Figure 8: Analysis of stem cell markers by qRT-PCR. Quantification of *PROM1*, *CD44, MSI1,* and *ALDH1a1* levels was performed on mRNA from spheroids at the indicated times. Histograms show mean ± standard deviation, n = 3, after normalization against *ACTB*. Data are represented as fold change relative to normal colon mucosa (red line = 1). NS: not significant; MS: marginally significant compared with D3, using unpaired Student's *t*-test. *: $P < 0.05$ compared with D3 or D5, using unpaired Student's *t*-test. Abbreviations: qRT-PCR = quantitative reverse transcription-

polymerase chain reaction; PROM1 = prominin-1; MSI1 = Musashi 1; ALDH1α1 = aldehyde dehydrogenase 1 alpha; ACTB = β-actin.

Figure 9: Effect of chemotherapy on spheroids. After harvesting from the microwells, spheroids were cultured in agarose-coated plates and treated for 3 days with FOLFOX or FOLFIRI or were maintained in (control) non-treated (NT) condition. (**A**) Analysis of fluorescence due to labeling of nucleic acid in dead cells. Histograms show mean ± standard deviation (SD), n = 4. (**B**) Morphological features of the spheroids maintained in the different culture conditions. Images were taken with a 4x objective. Scale bar: 400 μm. (**C**) Quantification of *PROM1*, *MSI1,* and *ALDH1α1* mRNAs by qRT-PCR. Histograms show mean ± SD, n = 4, after normalization against *ACTB*. *: NS: not significant; P < 0.05; **: P < 0.01; ***: P < 0.001 compared to the control (NT) condition, using unpaired Student's *t*-test. Abbreviations: FOLFOX = 5-Fluorouracil, 50 μg/mL; Oxaliplatin, 10 μg/mL; Leucovorin, 25 μg/mL ; FOLFIRI = 5-Fluorouracil, 50 μg/mL; Irinotecan, 100 μg/mL; Leucovorin, 25 μg/mL; qRT-PCR = quantitative reverse transcription-polymerase chain reaction; PROM1 = prominin-1; MSI1 = Musashi 1; ALDH1α1 = aldehyde dehydrogenase 1 alpha; ACTB = β-actin.

Table 1: Summary of spheroid formation and cell seeding.

Table 2: Volumes of agarose solution for coating of different plates/dishes.

Table 3: Primers used for quantitative reverse transcription-polymerase chain reaction.

DISCUSSION:

In vitro 3D models overcome the main experimental drawbacks of 2D cancer cell cultures, as they appear to be more reliable in recapitulating typical tumoral features including microenvironment and cell heterogeneity. Commonly used 3D models of spheroids are scaffold-free (cultured in low-attachment conditions) or scaffold-based (using biomaterials to culture cells). These methods present different disadvantages as they depend on the nature of the scaffold used or give rise to spheroids that are variable in structure and size.

The present protocol reports optimized conditions for producing homogeneous spheroids from the colon adenocarcinoma cell line, Caco2, by using a scaffold-free method. The spheroids are easily harvested and contrary to a previously reported study[41], they grow successfully and their growth characteristics during the time in culture can also be analyzed. Moreover, with this new method, the spheroids (a) actively proliferate, (b) present a very low rate of cell death, (c) organize to form a lumen inside the spheres, and (d) exhibit differentiation capacity of the component cells. Given that the final aim of the new approach was its use for studies on CSC biology, the expression of different markers of CSCs was analyzed. Interestingly, the markers presented a dynamic expression pattern depending on the time-point and defined different CSC populations.

Of utmost importance, the spheroids generated through this protocol could be used for analyzing drugs relevant for clinical applications such as the chemotherapeutic regimens, FOLFOX and FOLFIRI. The results also underline a heterogeneous response of cells to the drugs depending on the CSC marker analyzed. This observation is consistent with the current view that heterogeneous and multiple CSC-like cell populations within tumors display diverse chemosensitivity/chemoresistance properties[42,43]. This finding strongly potentiates the applicability of this new method for large scale screening. In addition to the applications reported in this study, the new protocol can also be used for a wider range of analyses (e.g., RNA and/or DNA extraction and large-scale analyses, western blotting, and immunofluorescence). Indeed, the volume of spheroids and growth characteristics can be easily determined by applying the sphere volume formula which, if necessary, also takes into consideration different diameters to counterbalance deviations from a perfectly spherical form. However, specific parameters should be optimized depending on the cell type (cell line or fresh primary cultures) and growth capacity such as the replication time. Nevertheless, the protocol indicates critical steps that can be easily adjusted.

Some points of concern need to be considered when carrying out spheroid generation described in this article. First, several washing steps should be performed with the anti-adherence rinsing solution to promote the homogeneity and compaction of the spheres. In this case, two washes were necessary. Second, bubbles must be removed from the microwells as this can disturb the correct formation of the spheroids. Third, once the cells are seeded in each microwell after the centrifugation step, the plate must remain undisturbed for two days. Additional considerations and changes in the protocol are needed when studying the early steps of spheroid formation, possibly including an automated visualization and imaging system. Fourth, changing the medium without disturbing the spheroids, given that they are in suspension, can be challenging. Hence, it is recommended to change only half of the volume each time. Fifth, when harvesting the spheroids, it is important to preserve their structure. Hence, the use of serological pipettes or micropipettes with the tips cut off is recommended for all dispensing steps after rinsing in a serum-containing medium or PBS to prevent the spheroids from adhering to the tips.

Some limitations may also be encountered when using this protocol. First, not all cell lines or cell types have the same culture parameters; in some cases, cell heterogeneity and the number of passages/aging of cells may also affect the ability to form spheroids. Second, similar to organoids, it may be difficult to maintain spheroids for a very long time in culture. In addition, it may not be feasible to replicate spheroids by simple fragmentation through a micropipette tip[15]. Third, this protocol cannot be adapted for single-spheroid analysis because manually recovering spheroids one by one can be tricky. This technique is more suitable for obtaining high amounts of homogeneous spheroids at the same time. Finally, for studies investigating the effects of growth factors originating from other cell types or analyzing the importance of the microenvironment, it would be important to enrich the model and perform co-culture experiments.

In conclusion, the present methodology describes a new protocol to efficiently generate and culture spheroids from Caco2 cells. The results demonstrate that this method can be applied to the study of tumor heterogeneity and for the analysis of CSCs. This method can also be used for

high-throughput drug screening and the study of stem cell biology in cancer and non-cancerous cells.

ACKNOWLEDGMENTS:

We acknowledge the imaging and Anipath recherche histology platforms (CRCL, CLB). We are indebted to the pharmacy of the Centre Léon Bérard (CLB) Hospital for the kind gift of FOLFOX and FOLFIRI. We also thank Brigitte Manship for critical reading of the manuscript. The work was supported by the FRM (Equipes FRM 2018, DEQ20181039598) and by the Inca (PLBIO19-289). MVG and LC received support from the FRM and CF received support from ARC foundation and the Centre Léon Bérard.

DISCLOSURES:

The authors have nothing to disclose

REFERENCES:

1. Bray, F. et al. Global cancer statistics 2018: GLOBOCAN estimates of incidence and mortality worldwide for 36 cancers in 185 countries. *CA: A Cancer Journal for Clinicians*. **68** (6), 394–424 (2018).
2. Fearon, E. R., Vogelstein, B. A genetic model for colorectal tumorigenesis. *Cell*. **61** (5), 759–767 (1990).
3. Rao, C. V, Yamada, H. Y. Genomic instability and colon carcinogenesis: from the perspective of genes. *Frontiers in Oncology*. **3**, 130 (2013).
4. Fearon, E. R. Molecular genetics of colorectal cancer. *Annual Review of Pathology*. **6** (1), 479–507 (2011).
5. Tran, T. Q. et al. α-Ketoglutarate attenuates Wnt signaling and drives differentiation in colorectal cancer. *Nature Cancer*. **1** (3), 345–358 (2020).
6. Batlle, E., Clevers, H. Cancer stem cells revisited. *Nature Medicine*. **23** (10), 1124–1134 (2017).
7. Clevers, H. The cancer stem cell: premises, promises and challenges. *Nature Medicine*. **17** (3), 313–319 (2011).
8. Barker, N. et al. Crypt stem cells as the cells-of-origin of intestinal cancer. *Nature*. **457** (7229), 608–611 (2009).
9. Dutta, D., Heo, I., Clevers, H. Disease modeling in stem cell-derived 3D organoid systems. *Trends in Molecular Medicine*. **23** (5), 393—410 (2017).
10. Bleijs, M., van de Wetering, M., Clevers, H., Drost, J. Xenograft and organoid model systems in cancer research. *The EMBO Journal*. **38** (15), e101654–e101654 (2019).
11. Kawai, S. et al. Three-dimensional culture models mimic colon cancer heterogeneity induced by different microenvironments. *Scientific Reports*. **10** (1), 3156 (2020).

12. Ferreira, L. P., Gaspar, V. M., Mano, J. F. Design of spherically structured 3D in vitro tumor models -Advances and prospects. *Acta Biomaterialia*. **75**, 11–34 (2018).
13. Friedrich, J., Seidel, C., Ebner, R., Kunz-Schughart, L. A. Spheroid-based drug screen: considerations and practical approach. *Nature Protocols*. **4** (3), 309–324 (2009).
14. Chaicharoenaudomrung, N., Kunhorm, P., Noisa, P. Three-dimensional cell culture systems as an in vitro platform for cancer and stem cell modeling. *World Journal of Stem Cells*. **11** (12), 1065–1083 (2019).
15. Sato, T. et al. Single Lgr5 stem cells build crypt-villus structures in vitro without a mesenchymal niche. *Nature*. **459** (7244), 262–265 (2009).
16. Weiswald, L.-B., Bellet, D., Dangles-Marie, V. Spherical cancer models in tumor biology. *Neoplasia*. **17** (1), 1–15 (2015).
17. Nath, S., Devi, G. R. Three-dimensional culture systems in cancer research: Focus on tumor spheroid model. *Pharmacology & Therapeutics*. **163**, 94–108 (2016).
18. Silva-Almeida, C., Ewart, M.-A., Wilde, C. 3D gastrointestinal models and organoids to study metabolism in human colon cancer. *Seminars in Cell & Developmental Biology*. **98**, 98–104 (2020).
19. Chantret, I., Barbat, A., Dussaulx, E., Brattain, M. G., Zweibaum, A. Epithelial polarity, villin expression, and enterocytic differentiation of cultured human colon carcinoma cells: A survey of twenty cell lines. *Cancer Research*. **48** (7), 1936–1942 (1988).
20. Caro, I. et al. Characterisation of a newly isolated Caco-2 clone (TC-7), as a model of transport processes and biotransformation of drugs. *International Journal of Pharmaceutics*. **116** (2), 147–158 (1995).
21. Antonchuk, J. Formation of embryoid bodies from human pluripotent stem cells using AggreWell™ plates. *Methods in Molecular Biology*. **946**, 523–533 (2013).
22. Wolpin, B. M., Mayer, R. J. Systemic treatment of colorectal cancer. *Gastroenterology*. **134** (5), 1296-1310.e1 (2008).
23. Yaffee, P., Osipov, A., Tan, C., Tuli, R., Hendifar, A. Review of systemic therapies for locally advanced and metastatic rectal cancer. *Journal of Gastrointestinal Oncology*. **6** (2), 185–200 (2015).
24. Fujita, K., Kubota, Y., Ishida, H., Sasaki, Y. Irinotecan, a key chemotherapeutic drug for metastatic colorectal cancer. *World Journal of Gastroenterology*. **21** (43), 12234–12248 (2015).
25. Mohelnikova-Duchonova, B., Melichar, B., Soucek, P. FOLFOX/FOLFIRI pharmacogenetics: the call for a personalized approach in colorectal cancer therapy. *World Journal of Gastroenterology*. **20** (30), 10316–10330 (2014).
26. Jordan, N. J. et al. Impact of dual mTORC1/2 mTOR kinase inhibitor AZD8055 on acquired endocrine resistance in breast cancer in vitro. *Breast Cancer Research*. **16** (1), R12–R12 (2014).
27. Mohr, J. C. et al. The microwell control of embryoid body size in order to regulate cardiac differentiation of human embryonic stem cells. *Biomaterials*. **31** (7), 1885–1893 (2010).
28. Hughes, C. S., Postovit, L. M., Lajoie, G. A. Matrigel: A complex protein mixture required for optimal growth of cell culture. *Proteomics*. **10** (9), 1886–1890 (2010).
29. Luca, A. C. et al. Impact of the 3D microenvironment on phenotype, gene expression, and EGFR inhibition of colorectal cancer cell lines. *PLoS One*. **8** (3), e59689 (2013).
30. Petersen, O. W., Rønnov-Jessen, L., Howlett, A. R., Bissell, M. J. Interaction with basement membrane serves to rapidly distinguish growth and differentiation pattern of normal and

malignant human breast epithelial cells. *Proceedings of the National Academy of Sciences of the United States of America*. **89** (19), 9064–9068 (1992).
31. Nusse, R., Clevers, H. Wnt/β-catenin signaling, disease, and emerging therapeutic modalities. *Cell*. **169** (6), 985–999 (2017).
32. Sambuy, Y., De Angelis, I., Ranaldi, G., Scarino, M. L., Stammati, A., Zucco, F. The Caco-2 cell line as a model of the intestinal barrier: influence of cell and culture-related factors on Caco-2 cell functional characteristics. *Cell Biology and Toxicology*. **21** (1), 1–26 (2005).
33. Vermeulen, L., Snippert, H. J. Stem cell dynamics in homeostasis and cancer of the intestine. *Nature Reviews Cancer*. **14** (7), 468–480 (2014).
34. van der Heijden, M., Vermeulen, L. Stem cells in homeostasis and cancer of the gut. *Molecular Cancer*. **18** (1), 66 (2019).
35. Barker, N., Bartfeld, S., Clevers, H. Tissue-resident adult stem cell populations of rapidly self-renewing organs. *Cell Stem Cell*. **7** (6), 656–670 (2010).
36. van der Flier, L. G., Haegebarth, A., Stange, D. E., van de Wetering, M., Clevers, H. OLFM4 is a robust marker for stem cells in human intestine and marks a subset of colorectal cancer cells. *Gastroenterology*. **137** (1), 15–17 (2009).
37. Potten, C. S. et al. Identification of a putative intestinal stem cell and early lineage marker; musashi-1. *Differentiation*. **71** (1), 28–41 (2003).
38. Clevers, H. The intestinal crypt, a prototype stem cell compartment. *Cell*. **154** (2), 274–284 (2013).
39. Clark, D. W., Palle, K. Aldehyde dehydrogenases in cancer stem cells: potential as therapeutic targets. *Annals of Translational Medicine*. **4** (24), 518 (2016).
40. Tomita, H., Tanaka, K., Tanaka, T., Hara, A. Aldehyde dehydrogenase 1A1 in stem cells and cancer. *Oncotarget*. **7** (10), 11018–11032 (2016).
41. Zoetemelk, M., Rausch, M., Colin, D. J., Dormond, O., Nowak-Sliwinska, P. Short-term 3D culture systems of various complexity for treatment optimization of colorectal carcinoma. *Scientific Reports*. **9** (1), 7103 (2019).
42. Garcia-Mayea, Y., Mir, C., Masson, F., Paciucci, R., LLeonart, M. E. Insights into new mechanisms and models of cancer stem cell multidrug resistance. *Seminars in Cancer Biology*. **60**, 166–180 (2020).
43. Marusyk, A., Janiszewska, M., Polyak, K. Intratumor heterogeneity: The Rosetta Stone of therapy resistance. *Cancer Cell*. **37** (4), 471–484 (2020).

Figure 1

A

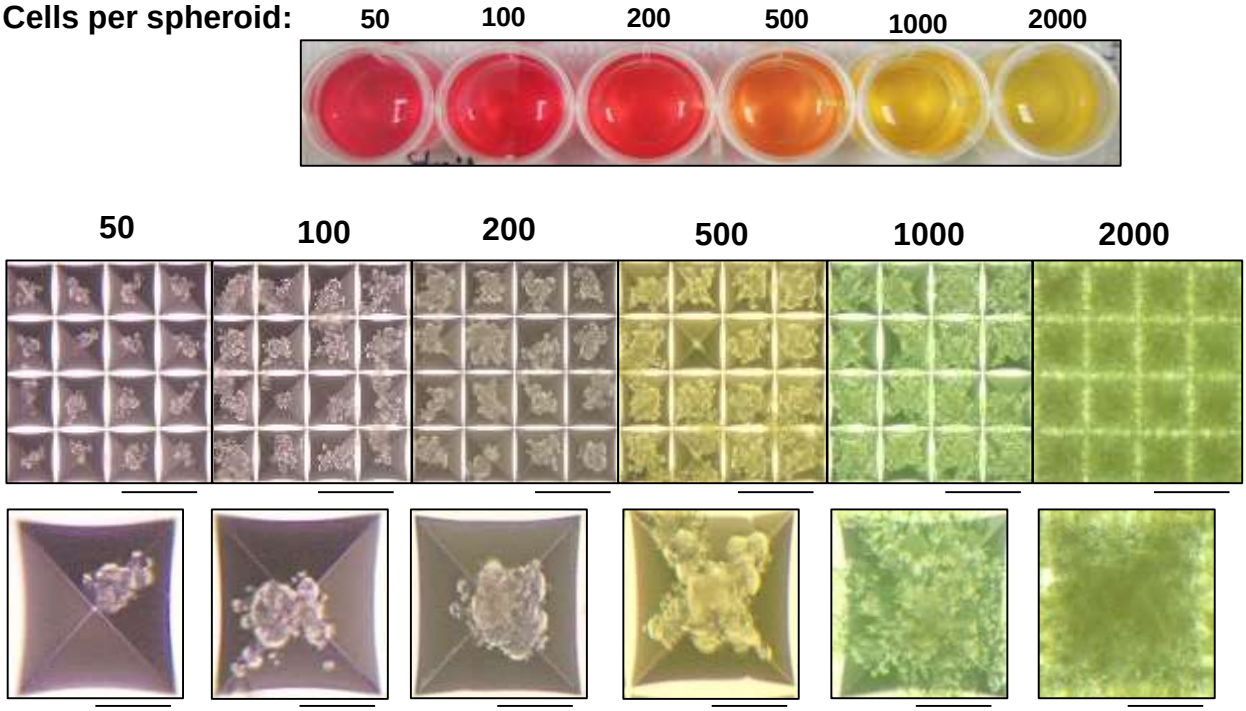

B

$$\text{Estimated volume } (\mu m^3) = \frac{4}{3}\pi\left(\frac{d_1}{2}\frac{d_2}{2}\frac{d_3}{2}\right)$$

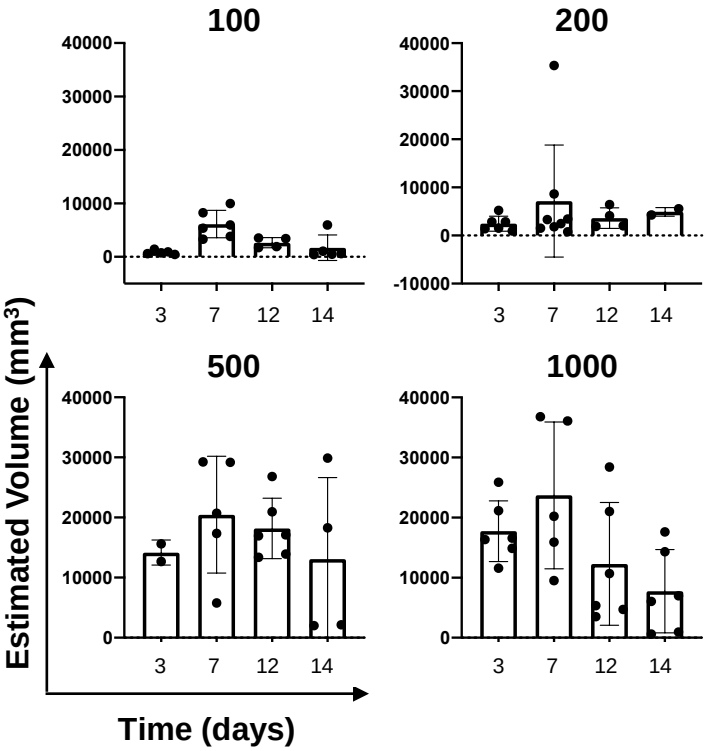

Figure 2

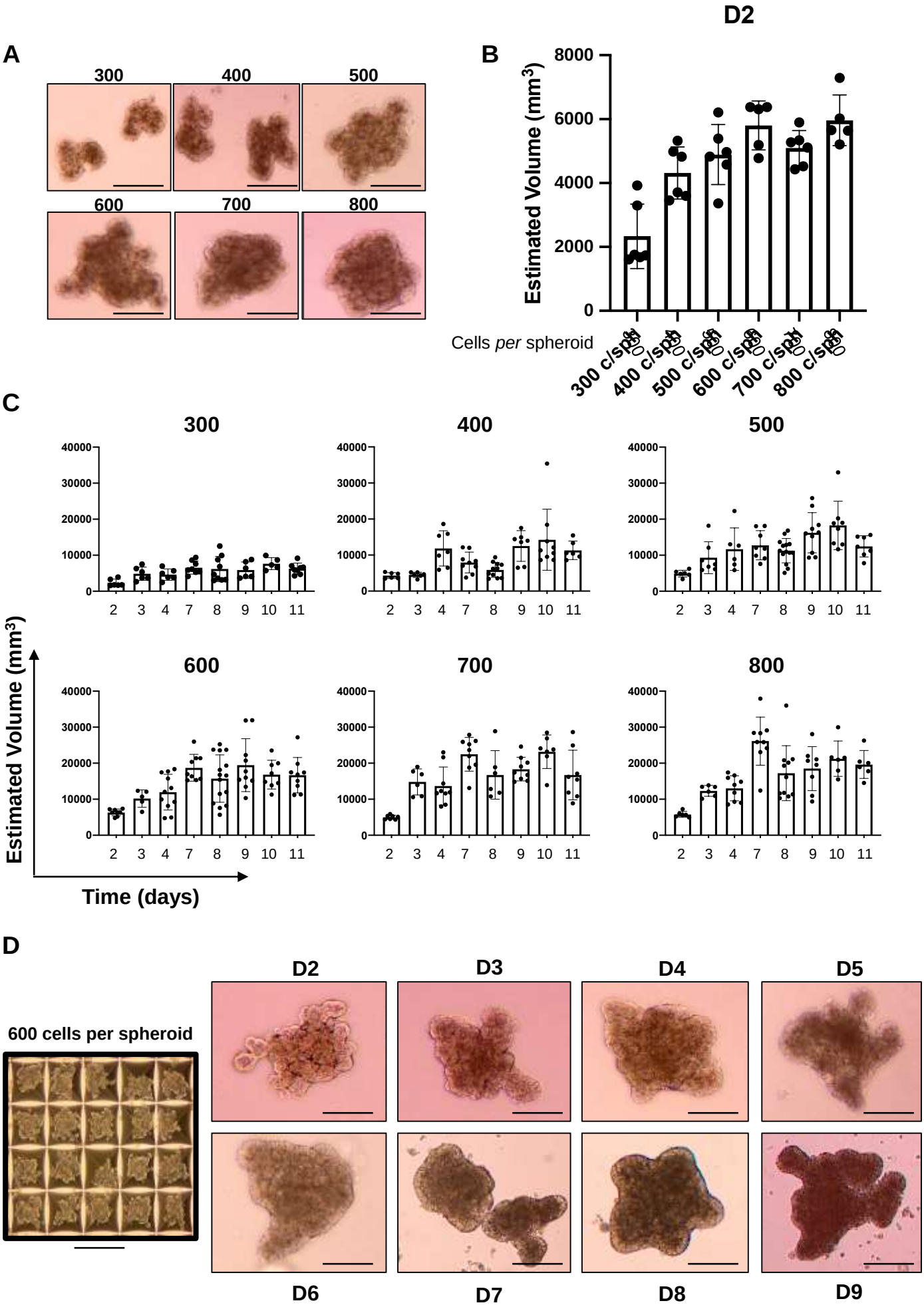

Figure 3

D3

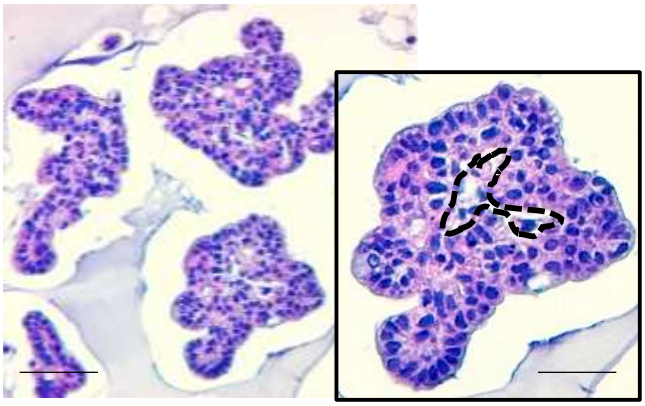

D5

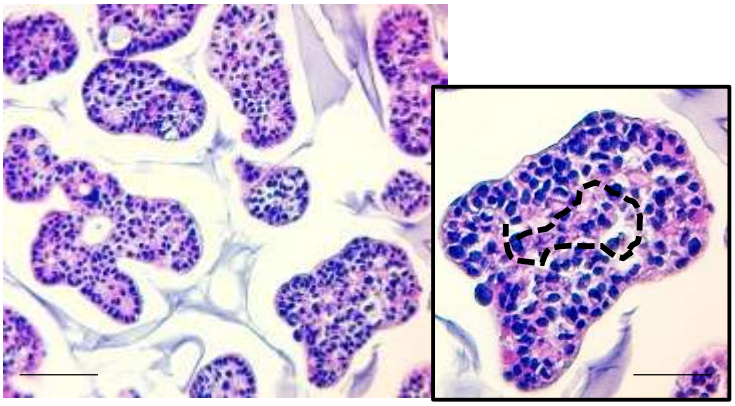

D7

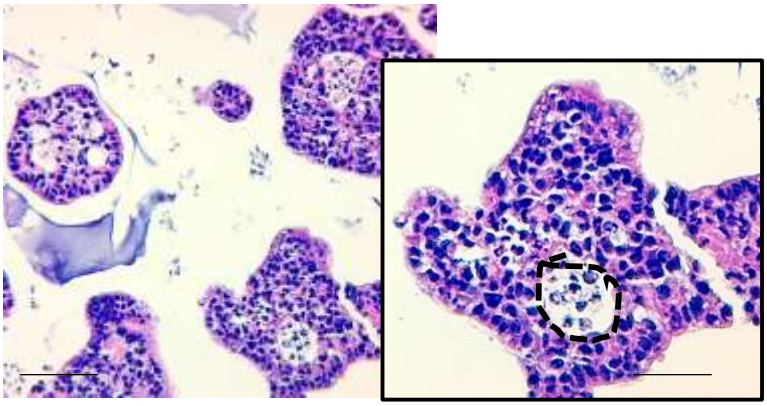

D10

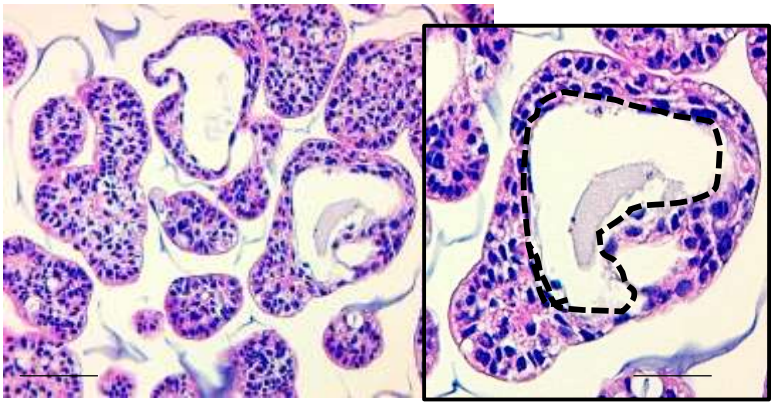

Figure 4

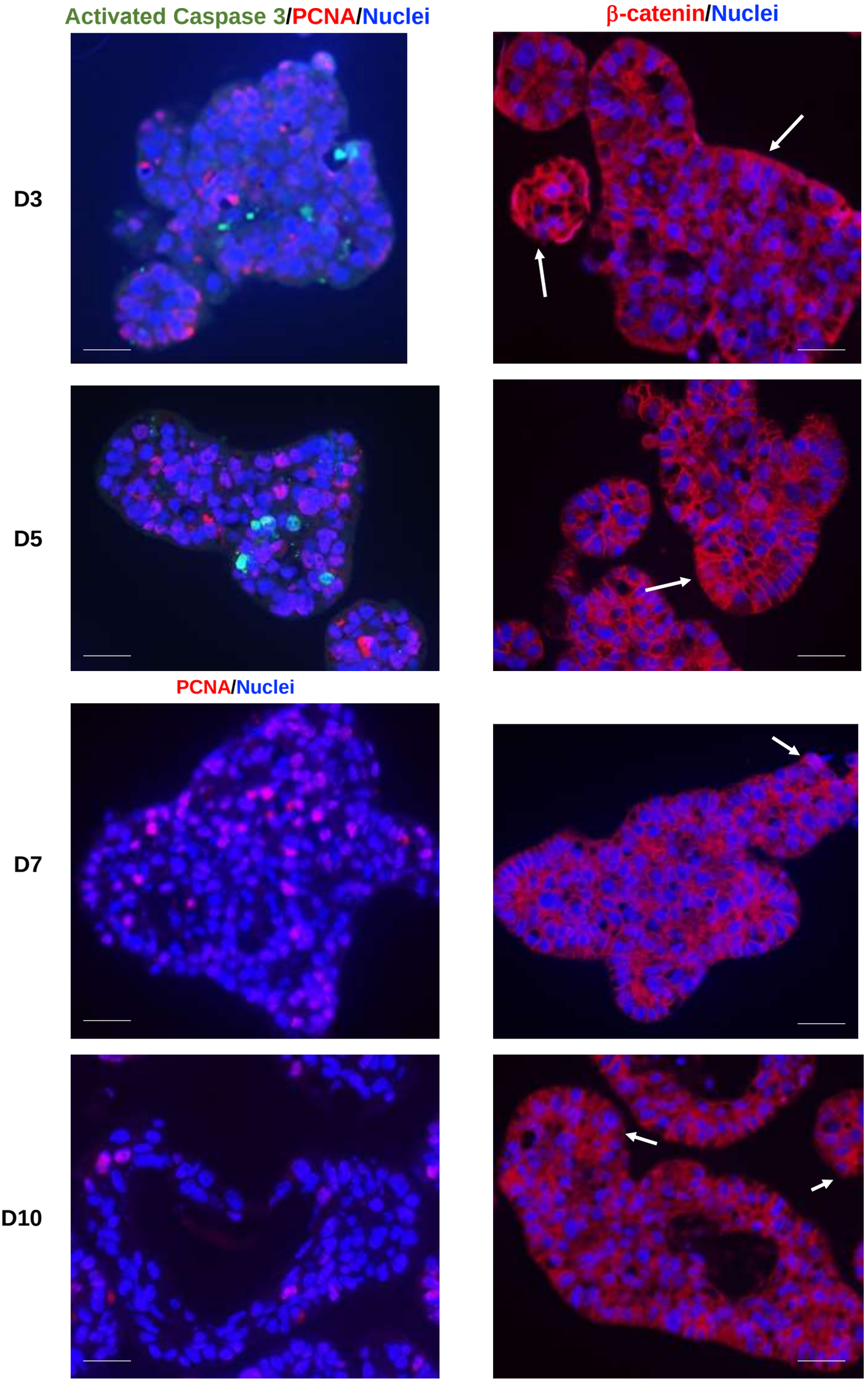

Figure 5

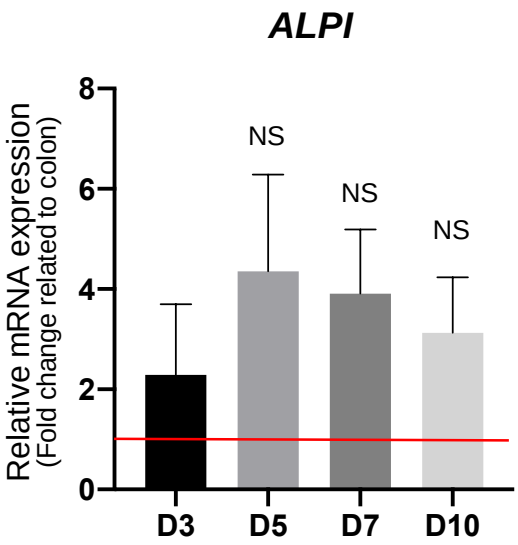

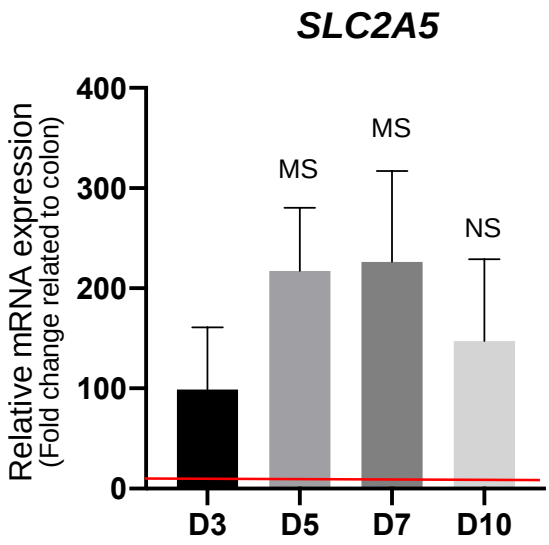

Figure 6

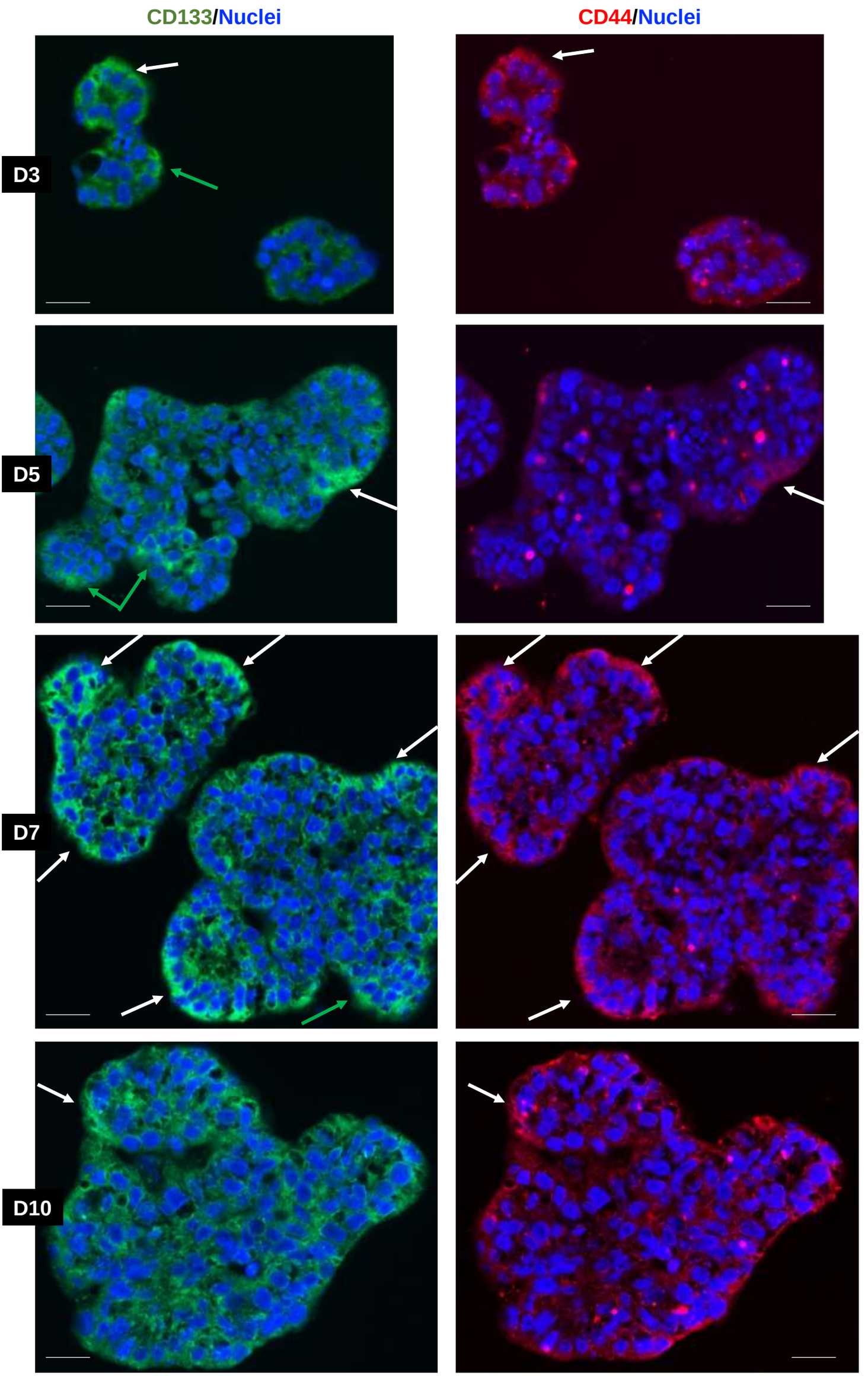

Figure 7

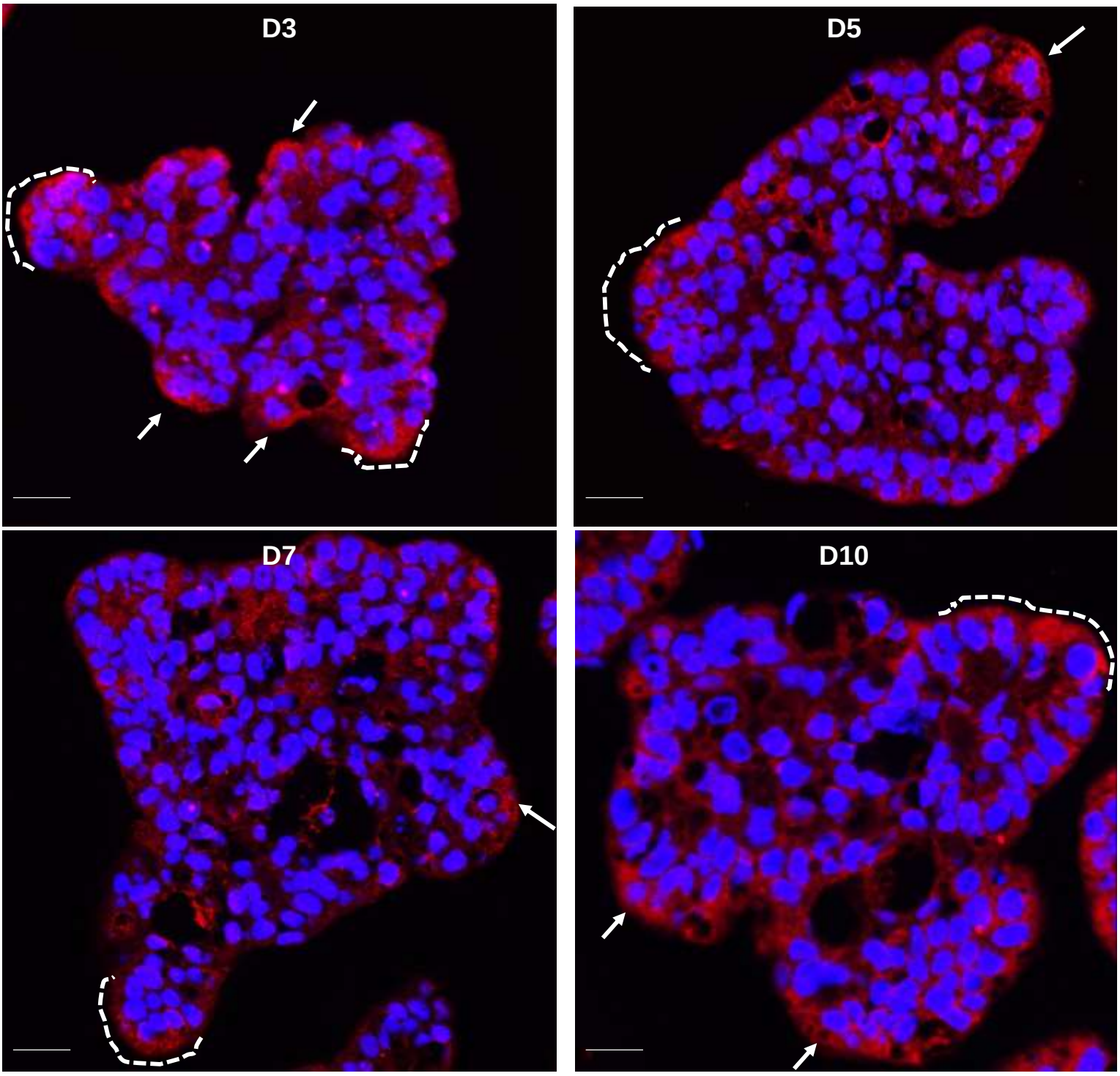

Figure 8

Click here to access/download;Figure;Figure 8.pdf

Figure 8

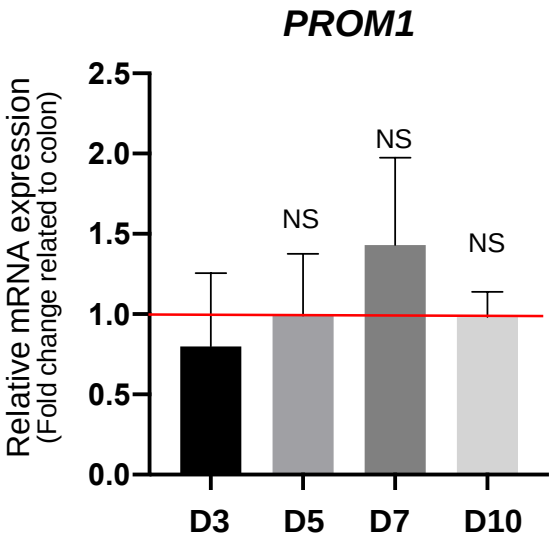

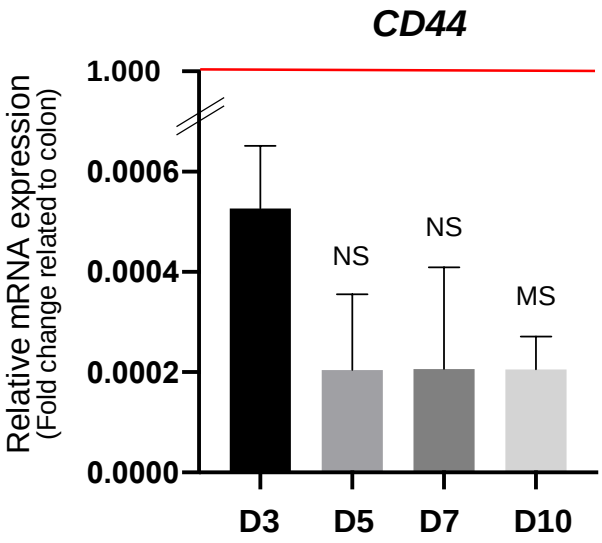

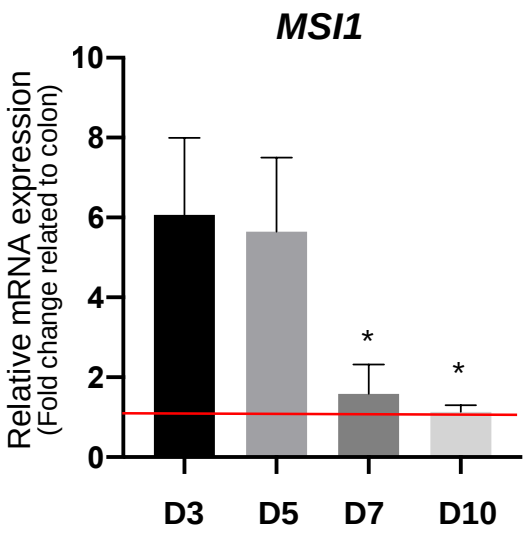

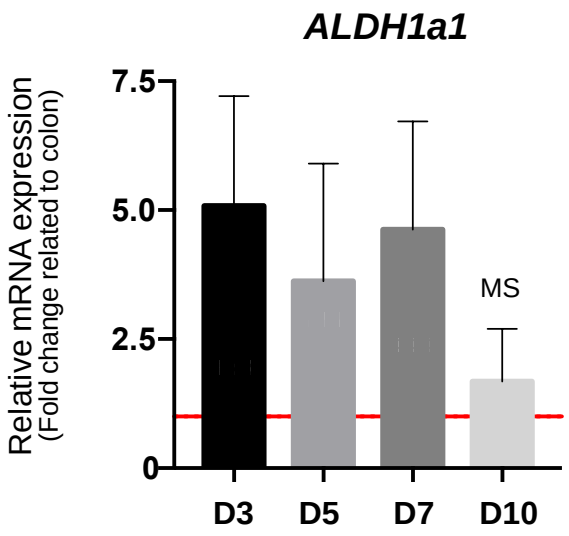

Click here to access/download;Figure;Figure 9.pdf

Figure 9

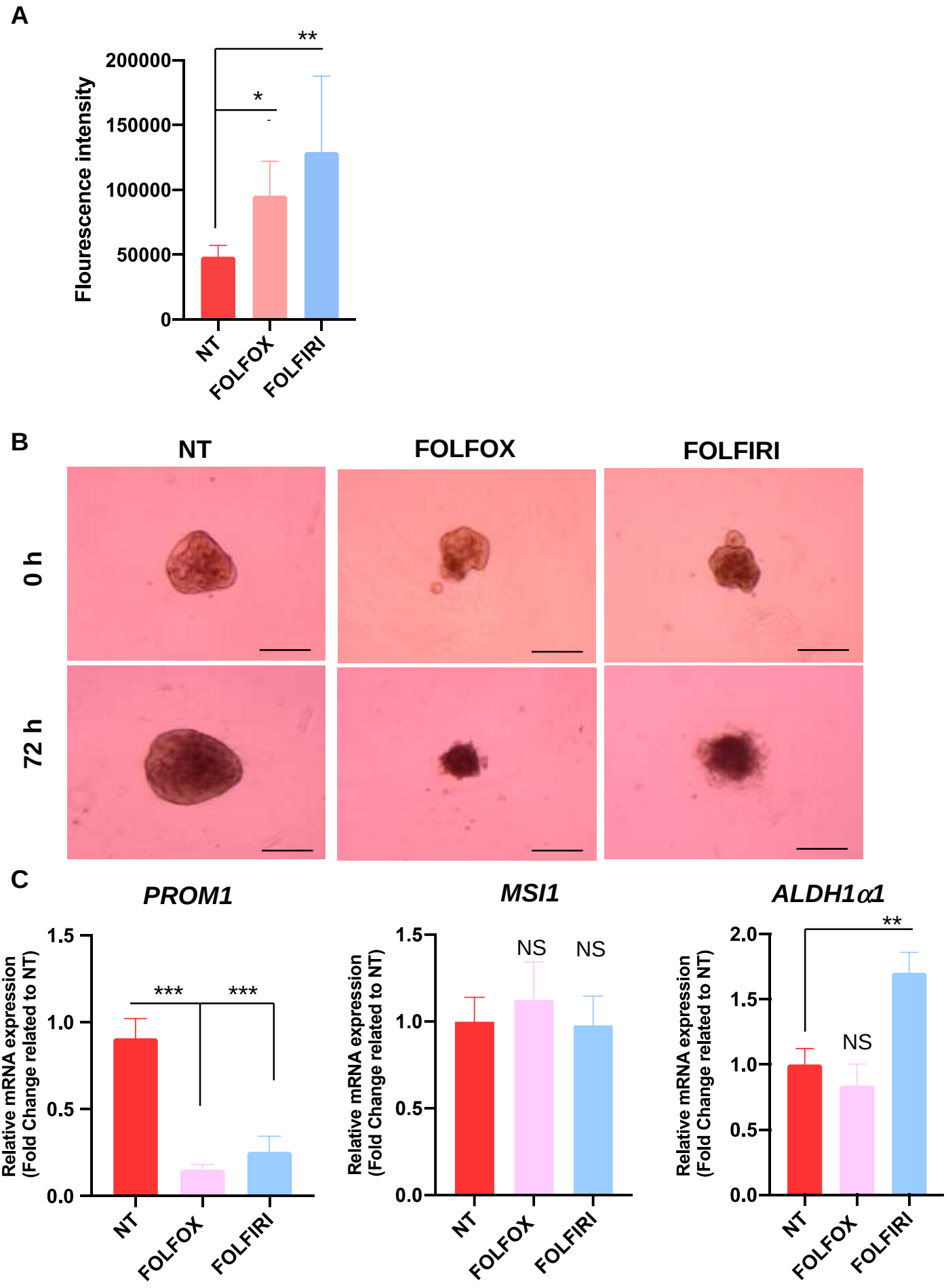

Table 1

Desired number of cells per spheroid	Required number of cells per well
50	6×10^4
100	1.2×10^5
200	2.4×10^5
300	3.6×10^5
400	4.8×10^5
500	6×10^5
600	7.2×10^5
700	8.4×10^5
800	9.6×10^5
1000	1.2×10^6
2000	2.4×10^6

Table 2

	10 mm dishes	6-well plates	12-well plates
Coating Volume	4 mL	300 µL	250 µL

24-well plates	96-well plates
150 µL	50 µL (Down & Up)

Table 3

	Genes	Primers
Differentiation markers	*ALPI*	Forward
		Reverse
	SLC2A5	Forward
		Reverse
Stem cell markers	*ALDH1a1*	Forward
		Reverse
	MSI1	Forward
		Reverse
	PROM1	Forward
		Reverse
	CD44	Forward
		Reverse
	OLFM4	Forward
		Reverse
Housekeeping genes	*ACTB*	Forward
		Reverse
	PPIB	Forward
		Reverse

Sequence	Product Length
CTG GTA CTC AGA TGC TGA CA	81
ATG TTG GAG ATG AGC TGA GT	
TAC CCA TAC TGG AAG GAT GA	94
AAC AGG ATC AGA GCA TGA AG	
GCC TTC ACA GGA TCA ACA GAG	147
TGC AAA TTC AAC AGC ATT GTC	
AGT TGG CAG ACT ACG CAG GA	131
TGG TCC ATG AAA GTG ACG AAG	
GTA AGA ACC CGG ATC AAA AGG	131
GCC TTG TCC TTG GTA GTG TTG	
TGC CTT TGA TGG ACC AAT TAC	160
TGA AGT GCT GCT CCT TTC ACT	
TCT GTG TCC CAG TTG TTT TCC	118
ATT CCA AGC GTT CCA CTC TGT	
CAC CAT TGG CAA TGA GCG GTT C	134
AGG TCT TTG CGG ATG TCC ACG T	
ATG ATC CAG GGC GGA GAC TT	100
GCC CGT AGT GCT TCA GTT TG	

Table of Materials

Name of Material/ Equipment	Company	Catalog Number
37 µm Reversible Strainer, Large	STEMCELL Technologies	27250
5-Fluorouracil	Gift from Pharmacy of the Centre Leon Berard (CLB)	-
Agarose	Sigma	A9539
Aggrewell 400 24-well plates	STEMCELL Technologies	34411
Anti Caspase3 - Rabbit	Cell Signaling	9661
Anti Musashi-1 (14H1) - Rat	eBioscience/Thermo Fisher	14-9896-82
Anti-Adherence Rinsing Solution x 100 mL	STEMCELL Technologies	07010
Anti-CD133 (13A4) - Rat	Invitrogen	14-133-82
Anti-CD44 -Rabbit	Abcam	ab157107
Anti-PCNA - Mouse	Dako	M0879
Anti-β-catenin - Mouse	Santa Cruz Biotechnology	sc-7963
Black multiwell plates	Thermo Fisher Scientific	237108
Citric Acid Monohydrate	Sigma	C1909
CLARIOstar apparatus	BMG Labtech	
Dako pen		

Donkey anti-Mouse IgG (H+L) Secondary Antibody, Alexa Fluor 488	Thermo Fisher Scientific	A21202
Donkey anti-Mouse IgG (H+L) Secondary Antibody, Alexa Fluor 568	Thermo Fisher Scientific	A10037
Donkey anti-Rabbit IgG (H+L) Highly Cross-Adsorbed Secondary Antibody, Alexa Fluor 488	Thermo Fisher Scientific	A21206
Donkey anti-Rabbit IgG (H+L) Highly Cross-Adsorbed Secondary Antibody, Alexa Fluor 568	Thermo Fisher Scientific	A10042
Dulbecco's Modified Eagle Medium (DMEM) Glutamax (L-alanyl-L-glutamine dipeptide)	Gibco	10569010
Fetal Bovine Serum (FBS)	Gibco	16000044
Fluorogel mounting medium with DAPI	Interchim	FP-DT094B
Goat anti-Rat IgG (H+L) Cross-Adsorbed Secondary Antibody, Alexa Fluor 568	Thermo Fisher Scientific	A11077
ImageJ software		
Irinotecan	Gift from Pharmacy CLB	-
iScript reverse transcriptase	Bio-Rad	1708891
Leucovorin	Gift from Pharmacy CLB	-
Matrigel Basement Membrane Matrix	Corning	354234
Nucleospin RNA XS Kit	Macherey-Nagel	740902 .250
Oxaliplatin	Gift from Pharmacy CLB	-
Penicillin-streptomycin	Gibco	15140130
Phosphate Buffer Saline (PBS)	Gibco	14190250

SYBR qPCR Premix Ex Taq II (Tli RNaseH Plus)	Takara	RR420B
SYTOX- Green	Thermo Fisher Scientific	S7020
Trypsin-EDTA (0.05 %)	Gibco	25300062
Zeiss-Axiovert microscope		

Comments/Description
To be used with 50 mL conical tubes
stock solution, 5 mg/100 mL; final concentration, 50 µg/mL
1,200 microwells per well for spheroid formation and growth
dilution 1:200
dilution 1:500
dilution 1:100
dilution 1:2000
dilution 1:1000
dilution 1:50
microplate reader
marker pen to mark circles on slides for creating barriers for liquids

dilution 1:1000
dilution 1:1000
dilution 1:1000
dilution 1:1000
dilution 1:1000
Spheroid image analysis
stock solution, 20 mg/mL; final concentration, 100 µg/mL
stock solution, 50 mg/mL; final concentration, 25 µg/mL
Basement membrane matrix
stock solution, 100 mg/20 mL;final concentration, 10 µg/mL

nucleic acid stain; dilution 1:5000
inverted microscope for acquiring images of spheroids

Point-by-point responses to Editor and referees

We would like to thank the Editor and the referees for their generally positive comments and suggestions to improve the quality of our manuscript. We have provided below detailed responses to these comments.

All changes in the manuscript are highlighted in bold red characters.

Editorial comments:
Changes to be made by the Author(s):
1. Please revise the protocol highlighting to be 3 pages or less. This must include a one line space between the protocol substeps.

Re. We have controlled the length of the protocol (highlighted in yellow) and it is within the 3-page range.

2. Please discuss limitations in the Discussion.

Re. We have now included several limitations at the end of the discussion (pg. 14, lines 531-543).

_____
Reviewers' comments:
Reviewer #3:
Manuscript Summary:
This manuscript describes a protocol to develop 3D spheroids based on Caco-2 cells. The conventional 2D models have many limitations, and therefore many researchers are developing 3D models. Hence a detailed protocol to develop 3D models is interesting to readers.

Major Concerns:
A main concern is that the authors used Caco-2 cells. But Caco-2 cells are not homogenous, and could be changed after cultivation. Hence, what is the best passage for Caco-2 cells to develop 3D spheroids? Is there any thing special that researchers should pay attention to in order to develop reliable 3D models over time? Please specify.

Re. We have already commented on the choice and the use of Caco2 cells in the responses of the previous round of reviews. Briefly, depending on the time in 2D culture these cells have already been reported to differentiate[1,2], indicating that at low confluency they have a stem/progenitor-like potential. This point was of particular interest for us. In addition, although this is not mentioned in the paper because it is beyond its scope, one strong point for the use of Caco2 cells is related to our interest in studying the function of the thyroid hormones and their nuclear receptor TRa1 in intestinal stem and progenitor biology. As such, Caco2 cells have been successful used in our previous study[3], demonstrating that these cells have all the machinery necessary to integrate and respond to the signaling pathway we are interested in. Hence their use in this new protocol to produce spheroids.

Regarding their heterogeneity and possible changes during passage in culture, it is our general rule to avoid working with Caco2 cells older than passage 80, as it has been suggested in several studies[1, 2, 4, 5]. For this specific protocol, in order to ensure the repeatability of the experiments and the consistency of the results, we have used cells between passage 65 to 74. We applied the protocol several times for the current paper and we now use it routinely and constantly obtain spheroids with the same characteristics. We have not, however, used the protocol to analyze in detail up to which passage the phenotype is retained, because of the rule we mentioned above.
Thanks to the comment of the referee and in order to clarify this point and better guide the readers, we have now indicated at pg. 4 line 131, the number of the passages of cells that we consider convenient for the protocol. In addition, we have added a sentence in the discussion regarding a potential limitation of the protocol depending on the number of passaging/aging of cells (pg. 14 line 531-534).

Minor Concerns:
Normally, the 3D spheroid models should be spherical or nearly spherical. But the models in this manuscript appear to be not very spherical. How the sizes were measured?

Re. Depending on the cell line, spheroids may have a more or less spherical form[6]. Regarding the Caco2 cells, we are aware of the irregular form of the spheroids and this is why we applied a formula to measure volumes based on 3 principal diameters. This is indicated on the different sections of the paper: pg. 6, 8, 13 and Figure 1B.

Reviewer #4:
Manuscript Summary:
The authors describe a detailed method to reproducibly grow 3D spheroid cultures of Caco2 (human colon adenocarcinoma cell line). The method appears well described and should be easy to follow by other researchers. In the manuscript further characteristics of the Caco2 spheroids are outlined and demonstrate that this model can be used to study cancer stem cell biology in vitro.

Major Concerns:
none

Minor Concerns:
line 122: step 1.2.4-1.2.6
line 131: trypsin-EDTA
line 201; indicate the size of the pipette tip
line 324-Fig2D: also indicate size of scale bar in the figures

Re. These points have been corrected and/or indicated.

Line 345: would be useful and informative to show data of the differentiation markers chromogranin A, lysozyme or MUC 2 (perhaps as supplement)

Re. We thank the referee for this comment. Indeed, there was an error in the manuscript, as by immunolabeling we could not see any signal and this was also confirmed in preliminary RTqPCR tests indicating no amplification. We are sorry for the error that has now been corrected (pg.10, line 350). The observations were also in agreement with published studies, indicating a major potential of Caco2 cells to differentiate into enterocytes[1, 2].

Reviewer #5:
Minor Concerns:
**Authors followed the protocol of growing the spheroids in microwell plate for 2 days and then transferring them to agar coated well plate for long term culture. What was the advantage of this protocol over culturing the spheroids completely in agar coated plates?*

Re. As mentioned in the introduction and also commented during the protocol, the major advantages of using microwells are the standardization of the method to generate spheroids, the shorter time to obtain them and their more homogeneous size compared with other methods such as the "hanging drops". Because of the form of the microwells (inverted pyramids) the cells are retained at the apex of the pyramid in a small volume and upon proliferation the cells fuse and form an organized structure in a few days, in our case 48 hours.

**Authors claimed that with the addition of 2.5% matrigel to the DMEM complete medium helped in uniform spheroid formation. Authors may compare the spheroid growth chart with and without matrigel composition.*

Re. The results describe point-by-point steps we took in developing a well standardized protocol. Because each step gave specific indications, we did not systematically use the same conditions (number of cells to form spheroids) or collected and analyzed spheroids at same time points to advance in our protocol. The only common condition we can compare in terms of absence or presence of 2.5% Matrigel is 500 cells/microwell. Indeed, in the absence of Matrigel (Figure 1B) the size of the spheroids is more heterogeneous and it doubles from D3 to D7 but it then remains almost constant. In the case of Matrigel-added condition (Figure 2C), the size at each time point is more homogeneous and it increases more regularly with time in culture. We have now added a short comment on this point to the results section pg. 9, line 324-328.

**Figure 2D, images of the spheroids in second row were not labelled.*

Re. The error has been now corrected.

**Figure 4 and 6, images were not properly aligned.*

Re. We thank the referee for this comment. The images are not completely aligned essentially for two reasons: depending on the days in culture spheroids have very different sizes and, in the case of bigger spheroids, the selected images aim to better highlight the results and in some cases, this needs to include several spheroids. We have now reworked the images to have more homogeneous sizes and a better alignment.

Reviewer #6:
Manuscript Summary:
The manuscript and hence the described protocol is well-written and easy-to-follow.

Major Concerns:
no major concerns.

Minor Concerns:
I would include in the abstract and introduction the fact that the authors opt to produce 3D spheroids homogenous in size. This is first mentioned in the optimization experiments and is an important feature of the spheroid protocol.

Re. We thank the referee for this comment. We have now added the suggested phrase in both the abstract and introduction.

In fig. 9 the fluorescence experiment for the chemotherapeutic treatment show a strong decrease in spheroid diameter and cell morphology. Is this considered in the fluorescence intensity measurement? Are these data normalized to the number of cells? A fluorescence image would be useful.

Re. The analysis of fluorescence intensity was performed on intact spheroids, by using the CLARIOstar apparatus. Indeed, the dead cells within spheroids internalize the Sytox-green and the quantification of the fluorescence intensity was performed directly on the apparatus and in a black plate. The spheroids from the same experiment were then imaged by live inverted bright-field microscopy and the fluorescence intensity (cell death) quantified by the CLARIOstar. However, the referee is right in mentioning that we did not normalize the fluorescence intensity to the number of cells. As explained, the fluorescence was measured on intact spheroids and for each replicate we had 300 spheroids per agarose-coated well. Indeed, to be sure that in all replicates we analyzed a similar number of spheroids, at the moment of seeding we divided the total 1,200 spheroids from one well (each containing 1,200 microwells) into 4 agarose-coated wells. It is worth noting that the values in the replicates are very close, supporting our measurements even in the absence of normalization. Finally, because the whole experiment of spheroid formation, growth and treatment is lengthy and needs a great amount of materials for a consistent analysis, we specifically dedicated part of the spheroids to the quantification of the fluorescence intensity (CLARIOstar) instead of using them for imaging.

Bibliography

1. Chantret, I., Barbat, A., Dussaulx, E., Brattain, M.G., Zweibaum, A. Epithelial Polarity, Villin Expression, and Enterocytic Differentiation of Cultured Human Colon Carcinoma Cells: A Survey of Twenty Cell Lines. *Cancer Research*. **48** (7), 1936 LP – 1942, at <http://cancerres.aacrjournals.org/content/48/7/1936.abstract> (1988).
2. Sambuy, Y., De Angelis, I., Ranaldi, G., Scarino, M.L., Stammati, A., Zucco, F. The Caco-2 cell line as a model of the intestinal barrier: influence of cell and culture-related factors on Caco-2 cell functional characteristics. *Cell Biology and Toxicology*. **21** (1), 1–26, doi: 10.1007/s10565-005-0085-6 (2005).

3. Uchuya-Castillo, J. *et al.* Increased expression of the thyroid hormone nuclear receptor TRα1 characterizes intestinal tumors with high Wnt activity. *Oncotarget*. **9** (57), 30979–30996, doi: 10.18632/oncotarget.25741 (2018).
4. Briske-Anderson, M.J., Finley, J.W., Newman, S.M. The influence of culture time and passage number on the morphological and physiological development of Caco-2 cells. *Proceedings of the Society for Experimental Biology and Medicine*. **214** (3), 248–257, doi: 10.3181/00379727-214-44093 (1997).
5. Caro, I. *et al.* Characterisation of a newly isolated Caco-2 clone (TC-7), as a model of transport processes and biotransformation of drugs. *International Journal of Pharmaceutics*. **116** (2), 147–158, doi: https://doi.org/10.1016/0378-5173(94)00280-I (1995).
6. Ferreira, L.P., Gaspar, V.M., Mano, J.F. Design of spherically structured 3D in vitro tumor models -Advances and prospects. *Acta biomaterialia*. **75**, 11—34, doi: 10.1016/j.actbio.2018.05.034 (2018).

CRCL CENTRE DE RECHERCHE EN CANCÉROLOGIE DE LYON

Lyon, 25 November 2020

JoVE Editor,

Dear Sir or Madam:

On behalf of my co-authors, I would like to submit the revised manuscript JoVE61783R1 entitled "**Establishing a new and reliable 3D model of spheroids to study colon cancer stem cells**".

After careful consideration of all the comments and concerns of the Editor and the referees, we have modified our paper to address these constructive comments. The modifications are detailed in the point-by-point responses to the Editor and referees.

We appreciate the suggestions and comments of the Editor and referees and believe that the manuscript has now been greatly improved and deserves consideration for publication in JoVE.

Thank you for giving us the opportunity to submit a revised manuscript.

Yours sincerely,

Dr Michelina Plateroti, *PhD*
Team: Development, cancer and stem cells
Cancer Research Center of Lyon
UMR Inserm 1052 - CNRS 5286 – University Lyon 1
28 rue Laennec
Lyon, France